Regioselective Ortho Palladation of Stabilized Iminophosphoranes in Exo Positions: Scope, Limitations, and Mechanistic Insights

David Aguilar,[†] Raquel Bielsa,[†] María Contel,[‡] Agustí Lledós,*[,§] Rafael Navarro,[†] Tatiana Soler,[||] and Esteban P. Urriolabeitia*[,†]

Departmento de Compuestos Organometálicos, ICMA, Universidad de Zaragoza-CSIC, Plaza S. Francisco s/n, E-50009 Zaragoza, Spain, Chemistry Department, Brooklyn College and The Graduate Center (CUNY), 2900 Bedford Avenue, Brooklyn, New York 11210, Departament de Química, Edifici C.n, Universitat Autònoma de Barcelona, 08193 Bellaterra, Barcelona, Spain, and Servicios Técnicos de Investigación, Facultad de Ciencias Fase II, Universidad de Alicante, 03690 San Vicente de Raspeig, Alicante, Spain

Received November 23, 2007

The reactivity of the stabilized iminophosphoranes $R_3P{=}NC(O)Ph$ (R = *p*-tolyl, *m*-tolyl), $Ph_3P{=}NC(O)CH_2Ph$, and $Ph_2P(CH_2)_nPPh_2{=}NC(O)Ph$ (n = 1, 2) toward $Pd(OAc)_2$ has been examined. These substrates undergo palladation at the ortho $C(sp^2)-H$ bond of the benzamide ring, giving exo complexes with complete regioselectivity. The mechanism of this reaction has been studied using DFT calculations and the regioselectivity explained on a kinetic basis, since the activation barrier is lower for the exo pathway than for the endo. The origin of this lower energy for the exo barrier seems to reside mainly on the interaction energy between the metal center and the ligand at the transition state. On the other hand, the palladation of the related keto-stabilized systems $Ph_3P{=}NC(O)FG$ (FG = NC_4H_8, NC_4H_8O) gives selectively the endo isomers through C—H bond activation at the Ph ring of the PPh_3 unit.

Introduction

The metal-mediated CH bond activation reaction is recognized at present as being one of the most important research subjects, mainly due to its deep implications for the functionalization of organic molecules.[1] In this context, a selective activation—when several possibilities exist—is highly desirable, and synthetic strategies must be developed. For instance, when dealing with aromatic substrates, ortho functionalization is easily achieved through the introduction of an ancillary coordinating group on the starting substrate.[2] These reactions occur through the formation of ortho-metalated complexes, which are very valuable tools in stoichiometric and/or catalytic processes.[3] Following our current research in this field,[4] we have recently reported the selective ortho palladation of phosphorus ylides[5] and iminophosphoranes.[5,6] The results showed that both the stabilized P ylides $Ph_3P{=}CHC(O)Aryl$ and the nonstabilized iminophosphoranes $Me_nR_{3-n}P{=}NCH_2Aryl$ can be metalated: (i) at the R ring (phenyl or tolyl), giving endo derivatives; (ii) at the Aryl ring, giving exo complexes; (iii) even at both rings at the same time, this behavior being a function of the different substituents present in the molecule. The behavior of the stabilized iminophosphoranes $Ph_3P{=}NC(O)Aryl$ is quite more selective than that shown by the other substrates, since in all cases studied the palladation has been produced at the aryl ring directly bonded to the deactivating carbonyl group.[5] This selective exo metalation is remarkable, since endo metalation products seem to be more stable than the exo products on electronic grounds (metalloaromaticity),[7] although some controversy have appeared recently around this concept, on the basis

* To whom correspondence should be addressed. Fax: (+34) 976761187 (E.P.U.). E-mail: esteban@unizar.es (E.P.U.); agusti@klingon.uab.es (A.L.).
[†] Universidad de Zaragoza-CSIC.
[‡] Brooklyn College and The Graduate Center (CUNY).
[§] Universitat Autònoma de Barcelona.
[||] Universidad de Alicante.

(1) (a) Ryabov, A. D. *Synthesis* **1985**, 233. (b) Murai, S.; Kakiuchi, F.; Sekine, S.; Tanaka, Y.; Kamatani, A.; Sonoda, M.; Chatani, N. *Nature* **1993**, *366*, 529. (c) Dyker, G. *Angew. Chem., Int. Ed.* **1999**, *38*, 1698. (d) Rietling, V.; Sirlin, C.; Pfeffer, M. *Chem. Rev.* **2002**, *102*, 1731. (e) Goldberg, K. I.; Goldman, A. S., Eds. *Organometallic C—H Bond Activation; Activation and Functionalization of C—H Bonds*; American Chemical Society: Washington, DC, 2004; ACS Symposium Series 885. (f) Jones, W. D. *Inorg. Chem.* **2005**, *44*, 4475. (g) Godula, K.; Sames, D. *Science* **2006**, *312*, 67. (h) Deprez, N. R.; Sanford, M. S. *Inorg. Chem.* **2007**, *46*, 1924. (i) Bercaw, J. E.; Labinger, J. A. *Proc. Natl. Acad. Sci. U.S.A.* **2007**, *104*, 6899. (j) Chen, G. S.; Labinger, J. A.; Bercaw, J. E. *Proc. Natl. Acad. Sci. U.S.A.* **2007**, *104*, 6915.

(2) (a) Clegg, W.; Dale, S. H.; Hevia, E.; Honeyman, G. W.; Mulvey, R. E. *Angew. Chem., Int. Ed.* **2006**, *45*, 2370. (b) Clegg, W.; Dale, S. H.; Harrington, R. W.; Hevia, E.; Honeyman, G. W.; Mulvey, R. E. *Angew. Chem., Int. Ed.* **2006**, *45*, 2374.

(3) (a) Dupont, J.; Pfeffer, M.; Spencer, J. *Eur. J. Inorg. Chem.* **2001**, 1917. (b) Kakiuchi, F.; Murai, S. *Acc. Chem. Res.* **2002**, *35*, 826. (c) Kakiuchi, F.; Chatani, N. *Adv. Synth. Catal.* **2003**, *345*, 1077. (d) Bedford, R. B. *Chem. Commun.* **2003**, 1787. (e) van der Boom, M. E.; Milstein, D. *Chem. Rev.* **2003**, *103*, 1759. (f) Omae, I. *Coord. Chem. Rev.* **2004**, *248*, 995. (g) Farina, V. *Adv. Synth. Catal.* **2004**, *346*, 1553. (h) Schlummer, B.; Scholz, U. *Adv. Synth. Catal.* **2004**, *346*, 1599. (i) Beletskaya, I. P.; Cheprakov, A. V. *J. Organomet. Chem.* **2004**, *689*, 4055. (j) Dupont, J.; Consorti, C.; Spencer, J. *Chem. Rev.* **2005**, *105*, 2527. (k) Kalyani, D.; Deprez, N. R.; Desai, L. V.; Sanford, M. S. *J. Am. Chem. Soc.* **2005**, *127*, 7330. (l) Zapf, A.; Beller, M. *Chem. Commun.* **2005**, 431. (m) Daugulis, O.; Zaitsev, V. G.; Shavashov, D.; Pham, Q. N.; Lazareva, A. *Synlett* **2006**, 3382. (n) Vicente, J.; Abad, J. A.; López—Sáez, M. J.; Jones, P. G. *Organometallics* **2006**, *25*, 1851. (o) Hull, K. L.; Lanni, E. L.; Sanford, M. S. *J. Am. Chem. Soc.* **2006**, *128*, 14047. (p) Dick, A. R.; Sanford, M. S. *Tetrahedron* **2006**, *62*, 2439. (q) Daugulis, O.; Chiong, H. A. *Org. Lett.* **2007**, *9*, 1449.

(4) (a) Bielsa, R.; Larrea, A.; Navarro, R.; Soler, T.; Urriolabeitia, E. P. *Eur. J. Inorg. Chem.* **2005**, 1724. (b) Aguilar, D.; Contel, M.; Navarro, R.; Urriolabeitia, E. P. *Organometallics* **2007**, *26*, 4604.

(5) Aguilar, D.; Aragüés, M. A.; Bielsa, R.; Serrano, E.; Navarro, R.; Urriolabeitia, E. P. *Organometallics* **2007**, *26*, 3541.

(6) Bielsa, R.; Navarro, R.; Urriolabeitia, E. P.; Lledós, A. *Inorg. Chem.* **2007**, *46*, 10133.

(7) (a) Masui, H. *Coord. Chem. Rev.* **2001**, *219—221*, 957. (b) Ghedini, M.; Aiello, I.; Crispini, A.; Golemme, A.; La Deda, M.; Pucci, D. *Coord. Chem. Rev.* **2006**, *250*, 1373.

10.1021/om701174v CCC: $40.75
Publication on Web 05/31/2008

Scheme 1[a]

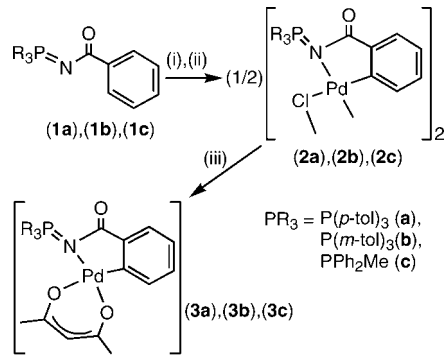

[a] Legend: (i) $Pd(OAc)_2/CH_2Cl_2/\Delta$; (ii) LiCl/MeOH; (iii) Tl(acac).

of NICS (nucleus-independent chemical shift) measurements.[8] On the other hand, the C−H bond activation produced at the phenyl ring of the benzamide group is also worth noting, due to the deactivating nature of the carbonyl substituent. A plausible explanation has been given, taking into account the resonant forms of the free ligand, since the presence of a negative charge delocalized around the NCO system could produce a more charged phenyl ring, in comparison with those at the PPh_3 phosphonium unit, and then a more favorable electrophilic substitution at the former.[5]

Aiming to obtain more insight about this very selective metalation, we have performed a detailed study of the ortho palladation of different stabilized iminophosphoranes. More specifically we have (a) changed the substituents at the phosphine group, (b) replaced the phosphine by a diphosphine ligand, and/or (c) introduced functional groups other than the aryl unit at the carbonyl moiety. Moreover, in order to shed light about on the ultimate reasons for the aforementioned selectivity, we have studied the mechanism of the ortho palladation of the model iminophosphorane $PhH_2P{=}NC(O)C_6H_5$, induced by $Pd(OAc)_2$, through DFT methods.

Results and Discussion

Ortho Palladation of $R_3P{=}NC(O)Ph$ and $Ph_3P{=}NC(O)CH_2Ph$. The starting iminophosphoranes $R_3P{=}NC(O)Ph$ (R_3P = P(*p*-tol)$_3$ (**1a**), P(*m*-tol)$_3$ (**1b**), PPh_2Me (**1c**)) have been prepared by following procedures reported by Pomerantz et al.,[9] while $Ph_3P{=}NC(O)CH_2Ph$ (**1d**) has been synthesized through the Staudinger method,[10] by reaction of PPh_3 with $N_3C(O)CH_2Ph$.[11] Attempts to prepare iminophosphoranes derived from P(*o*-tol)$_3$ failed, probably due to the particular steric requirements of this phosphine.

The reaction of **1a**−**c** with $Pd(OAc)_2$ (1:1 molar ratio) in refluxing CH_2Cl_2 and subsequent treatment of the acetate intermediate (not isolated) with excess LiCl in MeOH at room temperature give the dinuclear ortho-metalated derivatives **2a**−**c** as yellow solids (Scheme 1). Using different solvents or increasing the temperature of the reaction does not result in the formation of the endo isomer. The reaction of $Pd(OAc)_2$ with **1a**−**c** in refluxing toluene occurs with extensive decomposition, and only black Pd^0 was obtained. Complexes **2a**,**b** were obtained as single isomers (presumably trans), while **2c** was characterized as a 4/1 mixture of trans and cis isomers. The acetylacetonate derivatives **3a**−**c** have been prepared from reaction of **2a**−**c** with Tl(acac) (1:2 molar ratio) in order to increase the solubility of the compounds, to avoid the presence of isomers, and to properly characterize the metalated fragments. The spectroscopic data of **2a**−**c** and **3a**−**c** show unequivocally that the metalation has been produced regioselectively at the benzamide ring, giving exo derivatives. The ^{31}P NMR spectra show peaks in the 28 (**2a**,**b** and **3a**,**b**)−36 (**2c** and **3c**) ppm region: that is, showing a moderate downfield shift of the resonances, as expected for exo complexes.[5]

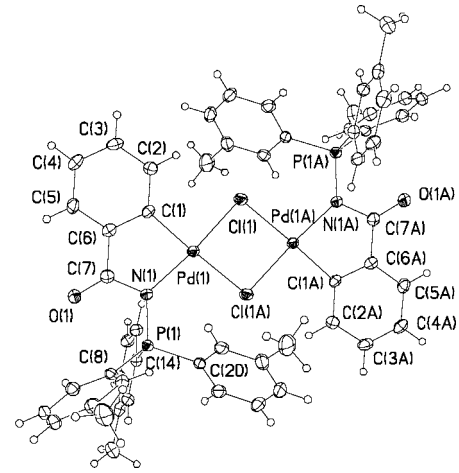

Figure 1. Thermal ellipsoid plot of complex **2b**. Non-hydrogen atoms are drawn at the 50% probability level.

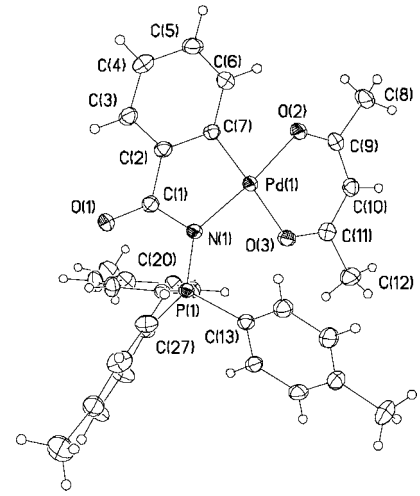

Figure 2. Thermal ellipsoid plot of complex **3a**. Non-hydrogen atoms are drawn at the 50% probability level.

The X-ray crystal structures of **2b** and **3a** have been determined. Figure 1 shows a molecular drawing of the dimeric compound **2b**, while that of **3a** is represented in Figure 2. Selected bond distances and angles are collected in Tables 1 (**2b**) and 2 (**3a**), and parameters concerning data solution and refinement are given in Table 3. The structure of **2b** shows a dinuclear complex, with two metalated fragments [Pd{C_6H_4-(C(O)N=P(*m*-tol)$_3$)-2}] bridged by two chlorine ligands, which is structurally analogous to examples previously reported.[5] The Pd1−C1 bond distance [1.979(2) Å] is slightly longer than those found in [Pd(μ-Cl){C_6H_3(Me-3)(C(O)N=PPh_3-2)}]$_2$ (1.962(3) Å)[5] and [Pd(C_6H_4(PPh_2=NC_6H_4Me-4′)-2)(μ-OAc)]$_2$ (1.964(3)

(8) Milci, M. K.; Ostojic, B. D.; Zaric, S. D. *Inorg. Chem.* **2007**, *46*, 7109.
(9) Bittner, S.; Assaf, Y.; Krief, P.; Pomerantz, M.; Ziemmnicka, B. T.; Smith, C. G. *J. Org. Chem.* **1985**, *50*, 1712.
(10) Staudinger, H.; Meyer, J. J. *Helv. Chim. Acta* **1919**, *2*, 635.
(11) Bräse, S.; Gil, C.; Knepper, K.; Zimmermann, V. *Angew. Chem., Int. Ed.* **2005**, *44*, 5188.

Table 1. Selected Bond Distances (Å) and Angles (deg) for Compound 2b

Pd1−C1	1.979(2)	Pd1−N1	2.085(2)
Pd1−Cl1	2.3233(7)	Pd1−Cl1A	2.4504(8)
P1−N1	1.644(2)	O1−C7	1.222(3)
N1−C7	1.390(3)	C6−C7	1.478(3)
C1−C2	1.387(3)	C1−C6	1.392(3)
C2−C3	1.385(4)	C3−C4	1.382(4)
C4−C5	1.384(4)	C5−C6	1.387(3)
C1−Pd1−N1	81.19(9)	C1−Pd1−Cl1	93.22(8)
N1−Pd1−Cl1A	102.79(6)	Cl1−Pd1−Cl1A	83.36(3)
Pd1−Cl1−Pd1A	96.64(3)	C7−N1−P1	115.83(17)
C7−N1−Pd1	113.22(15)	P1−N1−Pd1	129.49(11)
O1−C7−N1	123.7(2)	O1−C7−C6	124.0(2)
N1−C7−C6	112.3(2)		

Table 2. Selected Bond Distances (Å) and Angles (deg) for Compound 3a

Pd(1)−C(7)	1.961(2)	Pd(1)−O(2)	2.0304(15)
Pd(1)−N(1)	2.0695(16)	Pd(1)−O(3)	2.0787(15)
N(1)−C(1)	1.392(3)	N(1)−P(1)	1.6457(18)
C(1)−O(1)	1.227(3)	C(1)−C(2)	1.482(3)
C(2)−C(3)	1.393(3)	C(2)−C(7)	1.400(3)
C(3)−C(4)	1.384(3)	C(4)−C(5)	1.394(3)
C(5)−C(6)	1.395(3)	C(6)−C(7)	1.390(3)
C(8)−C(9)	1.502(3)	O(2)−C(9)	1.279(3)
C(9)−C(10)	1.392(3)	C(10)−C(11)	1.398(3)
C(11)−O(3)	1.262(3)	C(11)−C(12)	1.502(3)
C(7)−Pd(1)−O(2)	91.69(7)	C(7)−Pd(1)−N(1)	81.43(8)
O(2)−Pd(1)−O(3)	91.16(6)	N(1)−Pd(1)−O(3)	95.71(6)
C(1)−N(1)−P(1)	117.62(14)	C(1)−N(1)−Pd(1)	112.04(13)
P(1)−N(1)−Pd(1)	125.16(9)	O(1)−C(1)−N(1)	124.7(2)
O(1)−C(1)−C(2)	123.82(19)	N(1)−C(1)−C(2)	111.47(17)

and 1.959(3) Å),[12] while it is statistically identical with that found in [PdCl(C_6H_4(PPh_2=NC(O)-2-py-2)] (1.976(3) Å).[4a] In the same way, the Pd1−N1 bond distance (2.085(2) Å) is also longer than those found in the aforementioned complexes (range 1.997(2)−2.055(2) Å]).[4a,5,12] The two Pd1−Cl1 bond distances (2.3233(7) and 2.4504(8) Å) are different, indicating the different trans influences of the C_{aryl} and the iminic N atom,[13] but fall in the usual range of distances found for these types of complexes.[14] The P1−N1 bond distance (1.644(2) Å) is longer than that found in Ph_3P=NC(O)Ph (1.626(3) Å),[15] most probably due to the N bonding to the Pd center. A similar discussion can be carried out about internal parameters of the palladated ligand in [Pd{C_6H_4(C(O)N=P(*p*-tol)$_3$)-2}] (**3a**; Pd1−C7 = 1.961(2) Å; Pd1−N1 = 2.0695(16) Å, and P1−N1 = 1.6457(18) Å). The Pd1−O2 (2.0304(15) Å) and Pd1−O3 (2.0787(15) Å) bond distances fall in the usual range of distances found for chelating acac ligands.[14]

The palladation of **1a**−**c** has been produced regioselectively at the benzamide ring, as was observed in Ph_3P=NC(O)Aryl,[5] suggesting that the formation of exo isomers in this type of substrates could be a general process. The presence of methyl groups in the tolyl rings of the phosphine (**1a**,**b**) or, better, directly bonded to the phosphonium P atom (**1c**) should activate these rings toward an electrophilic substitution.[16] However, the expected activation does not seem to be enough to change the selectivity on the orientation of the reaction, since exo metalated compounds are also obtained. In our hands, the reasons for the observed behavior of **1a**−**c** could be the same as those invoked for the exo palladation of Ph_3P=NC(O)Aryl.[5]

More examples have been evaluated. Ph_3P=NC(O)CH_2Ph (**1d**) contains a CH_2 spacer between the amide function and the phenyl ring. In this way, the transmission of electronic effects from the amide group to the aryl ring becomes difficult and the size of the plausible palladacycles also becomes modified. The reaction of $Pd(OAc)_2$ with **1d** affords *trans*-[$PdCl_2${N(PPh_3)-C(O)CH_2Ph}$_2$] (**4**) (Scheme 2). However, the reaction of $Li_2[PdCl_4]$—another classical metalating reagent[17]—with **1d** (1:1 molar ratio) in MeOH/CH_2Cl_2 affords the cyclopalladated [Pd(μ-Cl){C_6H_4(CH_2C(O)N=PPh_3-κC,*N*)-2}]$_2$ (**2d**) via activation of the ortho CH bond of the phenylacetamide group (Scheme 2). The NMR characterization of **2d** shows that this complex is obtained as a mixture of cis and trans geometric isomers in a 1/7 molar ratio. The ^{1}H NMR spectrum shows peaks that belong to the PPh_3 fragment, as well as three signals (1/1/2 intensity) that may be assigned to the four protons of the palladated Pd($C_6H_4CH_2$) phenylacetamide group. Moreover, an AB spin system is observed for the diastereotopic CH_2 protons. The shape of these signals indicates that the molecular plane does not behave in **2d** as a symmetry plane. A detailed explanation should take into account that (i) a six-membered palladacycle is formed, (ii) the palladacycle must be notably warped, and (iii) it should be conformationally stable on the NMR time scale.[3j,18] The metalation of the benzyl ring in **1d** to give **2d** occurs easily under the usual ortho-palladation conditions. Complex **2d** displays a somewhat unusual six-membered-ring arrangement.[3f] This metalation is preferred over that involving the phenyl rings of the PPh_3 unit, which, in principle, should be a more likely option due to (i) the formation of a more stable five-membered ring, (ii) the endo effect, and (iii) the involvement of the same type of C(sp^2)−H bonds. These observations suggest that the metalation of a given ring comes from a delicate balance of several factors—endo effect, type of C(sp^n)−H bond, size of metallacycle, type, position, and nature of substituents—and that the consideration of only one of them is not a valid criterion.

Ortho Palladation of $Ph_2P(CH_2)_nPPh_2$=NC(O)Ph (n = 1, 2). The functionalized iminophosphoranes $Ph_2P(CH_2)_n$-PPh_2=NC(O)Ph (n = 1 (**1e**), 2 (**1f**)), derived from the bis-phosphines dppm (n = 1) and dppe (n = 2), have been obtained by reaction of $PhC(O)N_3$ with the corresponding bis-phosphine. The reaction was performed by careful dropwise addition of a solution of the azide to a solution of the bis-phosphine, ensuring an excess of phosphine with respect to the azide in the reaction medium during the addition to favor the formation of the monosubstituted derivative. Even with these precautions, some bis-iminophosphorane $(CH_2)_n$[Ph_2P=NC(O)-Ph]$_2$ (n = 1, 2) was detected in the respective crude products (almost 10% by NMR in the best cases). Fortunately, **1e**,**f** could be obtained as pure crystalline materials by column chromatographic purification of the crude products, using Et_2O/hexane mixtures as eluents (9/1 for **1e** and 7/3 for **1f**). The ^{31}P{^{1}H} NMR spectra show the presence of two doublets, one at about 22−25 ppm, assigned to the P nuclei of the P=N functional group, and the other one at very high field (from −12 to −25

(12) Vicente, J.; Abad, J. A.; Clemente, R.; López-Serrano, J.; Ramírez de Arellano, M. C.; Jones, P. G.; Bautista, D. *Organometallics* **2003**, *22*, 4248.
(13) (a) Coe, B.; Clenwright, S. J. *Coord. Chem. Rev.* **2000**, *203*, 5. (b) Zanini, M. L.; Meneghetti, M. R.; Ebeling, G.; Livotto, P. R.; Rominger, F.; Dupont, J. *Inorg. Chim. Acta* **2003**, *350*, 527.
(14) Orpen, A. G.; Brammer, L.; Allen, F. H.; Kennard, O.; Watson, D. G.; Taylor, R. *J. Chem. Soc., Dalton Trans.* **1989**, S1.
(15) Bar, I.; Bernstein, J. *Acta Crystallogr., Sect. B* **1980**, *36*, 1962.
(16) (a) Ryabov, A. D. *Chem. Rev.* **1990**, *90*, 403. (b) Canty, A. J.; van Koten, G. *Acc. Chem. Res.* **1995**, *28*, 406.
(17) Cope, A. C.; Friedrich, E. C. *J. Am. Chem. Soc.* **1968**, *90*, 909.
(18) Hiraki, K.; Fuchita, Y.; Takechi, K. *Inorg. Chem.* **1981**, *20*, 4316.

Table 3. Crystal Data and Structure Refinement Details for Compounds 2b, 2g·CHCl$_3$, and 3a

	2b	2g·CHCl$_3$	3a
empirical formula	$C_{56}H_{50}Cl_2N_2O_2P_2Pd_2$	$C_{47}H_{45}Cl_5N_4O_2P_2Pd_2$	$C_{33}H_{32}NO_3PPd$
fw	1128.62	1149.86	627.97
temp (K)	293(1)	293(1)	123(1)
radiation (λ, Å)	Mo Kα (0.710 73)	Mo Kα (0.710 73)	Mo Kα (0.710 73)
cryst syst	monoclinic	triclinic	monoclinic
space group	$P2_1/n$	$P\bar{1}$	$P2_1/c$
a (Å)	10.074(2)	10.6915(6)	10.62824(12)
b (Å)	11.086(2)	10.9268(6)	17.8907(2)
c (Å)	21.677(4)	20.5707(12)	15.85581(14)
α (deg)		101.123(1)	
β (deg)	99.54(3)	91.864(1)	105.5717(10)
γ (deg)		96.757(1)	
V (Å^3)	2387.5(8)	2337.9(2)	2904.25(5)
Z	2	2	4
D_{calcd} (Mg/m^3)	1.570	1.633	1.436
μ (mm^{-1})	0.978	1.167	0.728
cryst size (mm^3)	0.19 × 0.07 × 0.02	0.18 × 0.14 × 0.08	0.38 × 0.33 × 0.25
no. of rflns collected	20 904	18 164	52 246
no. of indep rflns	5221 (R_{int} = 0.0222)	8192 (R_{int} = 0.0829)	8428 (R_{int} = 0.0226)
no. of data/restraints/params	5221/0/301	8192/0/559	8428/0/357
goodness of fit on F^2	1.080	1.019	1.043
final R indices ($I > 2\sigma(I)$)	R1 = 0.0262	R1 = 0.0565	R1 = 0.0359
	wR2 = 0.0748	wR2 = 0.1566	wR2 = 0.0855
R indices (all data)	R1 = 0.0325,	R1 = 0.0617	R1 = 0.0443
	wR2 = 0.0760	wR2 = 0.1603	wR2 = 0.0894
largest diff peak, hole (e Å^{-3})	0.611, −0.291	1.807, −1.032	0.855, −0.515

Scheme 2[a]

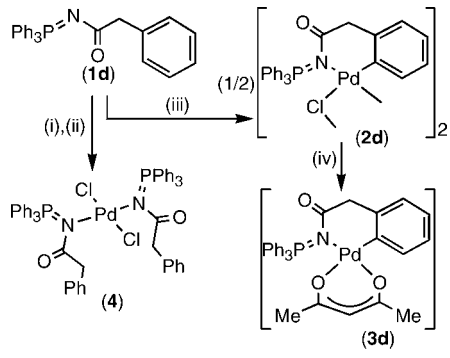

[a] Legend: (i) Pd(OAc)$_2$/CH$_2$Cl$_2$/Δ; (ii) LiCl/MeOH; (iii) Li$_2$[PdCl$_4$]/MeOH; (iv) Tl(acac).

ppm), assigned to the free PPh$_2$ moiety. These values are similar to those reported previously.[19]

Compounds **1e**,**f** react cleanly with Pd(OAc)$_2$ (1:1 molar ratio) and with an excess of LiCl (MeOH) to give the mononuclear species [Pd(Cl){C$_6$H$_4$(C(O)N=PPh$_2$(CH$_2$)$_n$PPh$_2$-κC,N,P)-2}] (n = 1 (**2e**), 2 (**2f**)) (eq 1). As expected, one of the ortho C−H bonds of the benzamide ring has been palladated and, in addition to the N bonding, the P coordination of the terminal PPh$_2$ moiety has taken place. In these compounds, this type of metalation was expected, since the competitive C−H bond activation at the phenyl rings of the N=PPh$_2$ group is very unlikely, due to steric constraints and the bonding of the terminal PPh$_2$ group. The trans arrangement of the P atom of the terminal PPh$_2$ unit and the palladated carbon atom is worth noting, evident from the observation of a large $^2J_{PC}$ coupling constant (about 140 Hz), since it should be very unfavorable due to the transphobia between these two groups.[20] In light of the preceding results it seems that, if a Ph ring is linked to the NC(O) or NC(O)CH$_2$ groups, the metalation is regioselectively oriented to this ring, giving exo derivatives. These results prompted us to investigate other types of substrates.

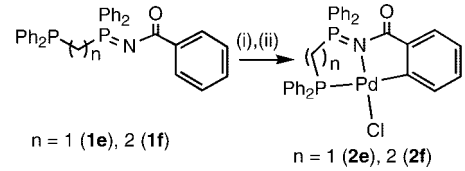

(1)

Ortho Palladation of Ph$_3$P=NC(O)FG (C(sp^2)/C(sp^3)). Two types of starting iminophosphoranes have been synthesized, by modification of the functional group linked to the C(O) group. One of them contains functional groups like *N*-pyrrolidine (NC$_4$H$_8$) (**1g**) or *N*-morpholine (NC$_4$H$_8$O) (**1h**) (eq 2). These are substrates in which a plausible metalation at the PPh$_3$ unit (C(sp^2)−H bond) would compete with that at the new heterocyclic unit (C(sp^3)−H bond). In the two cases five-membered metallacycles would be obtained. The other one contains functional groups such as 2-furan (**1i**) or 2-thiophene (**1j**), for which a C(sp^2)−H bond activation has been described previously.[21] Unfortunately, the palladation of **1i**,**j** was not successful, in spite of many modifications of the reaction conditions and/or the Pd source. In light of these results, **1i**,**j** were not further investigated.

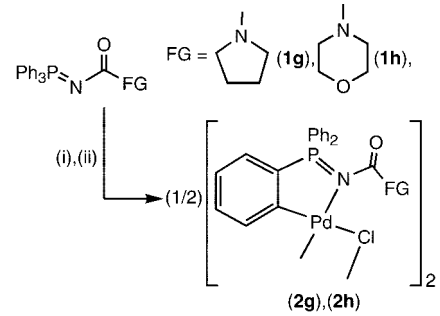

(2)

The synthesis of **1g**−**j** has been carried out through the Staudinger method, by reaction of the corresponding azide with

(19) (a) Katti, K. V.; Santarsiero, B. D.; Pinkerton, A. A.; Cavell, R. G. *Inorg. Chem.* **1993**, *32*, 5919. (b) Cadierno, V.; Crochet, P.; Díez, J.; García-Alvarez, J.; García-Garrido, S. E.; García-Granda, S.; Gimeno, J.; Rodríguez, M. A. *Dalton Trans.* **2003**, 3240. (c) Boubekeur, L.; Ricard, L.; Mézailles, N.; Le Floch, P. *Organometallics* **2005**, *24*, 1065.

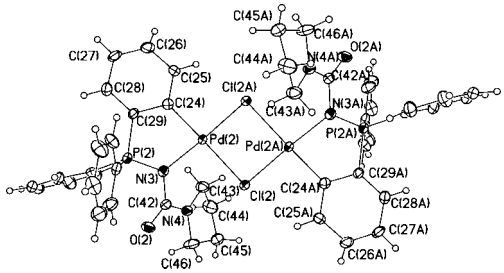

Figure 3. Thermal ellipsoid plot of complex **2g**. Non-hydrogen atoms are drawn at the 50% probability level.

PPh_3, and they have been characterized through the usual methods. **1g**,**h** react with $Pd(OAc)_2$ (1:1 molar ratio), in refluxing CH_2Cl_2, and with excess LiCl in MeOH to give the dinuclear $[Pd(\mu\text{-}Cl)\{C_6H_4(PPh_2{=}NC(O)NC_4H_8\text{-}\kappa C,N)\text{-}2\}]_2$ (**2g**) and $[Pd(\mu\text{-}Cl)\{C_6H_4(PPh_2{=}NC(O)NC_4H_8O\text{-}\kappa C,N)\text{-}2\}]_2$ (**2h**) derivatives, respectively (eq 2). In this case, the pattern of reactivity has been inverted, and one phenyl of the PPh_3 unit has undergone a CH bond activation process. While the presence of substituents on the phosphine moiety (**1a**−**c**) or the benzamide ring,[5] the size of the final palladacycle (**1d**), and the type of phosphine (**1e**,**f**) do not have a decisive influence over the outcome of the reaction, a change in the nature of the CH bond to be activated ($C(sp^2)$ vs $C(sp^3)$) seems crucial to decide the final orientation of the palladation. The structures of **2g**,**h** (endo) can be proposed on the basis of their NMR data and the X-ray structure of complex **2g**. The $^{31}P\{^1H\}$ NMR spectrum of **2g** shows a single peak at 42.53 ppm, while that of **2h** shows two peaks at 45.42 and 46.92 ppm. These chemical shifts are strongly shifted to low field with respect to those found for exo derivatives (range 29−32 ppm)[5] and are in good agreement with previous data reported for endo metalations.[4a] In addition, the number of peaks suggests that while **2g** is obtained as a single isomer, **2h** is probably a mixture of cis and trans geometric isomers.

The X-ray crystal structure of **2g** has been determined. A molecular drawing of **2g** is shown in Figure 3, selected bond distances and angles are collected in Table 4, and relevant parameters concerning data collection and structure solution are given in Table 3. There are two independent half-molecules in the asymmetric part of the unit cell, which are structurally analogous. Each independent molecule is a dinuclear complex, in which two units $[Pd\{C_6H_4(PPh_2{=}NC(O)NC_4H_8)\text{-}2\}]$ are bridged by two chlorine atoms. Within the dinuclear complex, each Pd atom is located in a distorted-square-planar environment, surrounded by the palladated carbon atom, the iminic N atom, and the two chlorine atoms. These facts show unambiguously the endo metalation of **1g**. In spite of the different ortho-palladation position—with respect to the exo complexes **2b** and **3a**—the Pd2−C24 bond distance (1.963(4) Å) is identical, within experimental error, with those found in these complexes (1.979(2) and 1.961(2) Å). The P2−N3 bond distance (1.6457(18) Å) is also identical (1.635(4) Å (**2g**); 1.644(2) Å (**2b**)). Only the Pd2−N3 bond distance (2.038(4) Å) appears to be slightly shorter than those found in **2b** and **3a** (Tables 1 and 2).

Theoretical Study of the Reaction Mechanism. In order to shed light on the regioselective metalation of iminophosphoranes

Table 4. Selected Bond Distances (Å) and Angles (deg) for Compound 2g·CHCl₃

Pd(2)−Cl(2A)	2.3240(11)	C(27)−C(28)	1.380(7)
Pd(2)−Cl(2)	2.4594(12)	C(28)−C(29)	1.396(6)
Pd(2)−C(24)	1.963(4)	N(3)−C(42)	1.386(6)
Pd(2)−N(3)	2.038(4)	C(42)−N(4)	1.346(6)
N(3)−P(2)	1.635(4)	C(42)−O(2)	1.234(5)
P(2)−C(29)	1.782(5)	N(4)−C(43)	1.467(6)
C(29)−C(24)	1.420(6)	C(43)−C(44)	1.534(7)
C(24)−C(25)	1.404(6)	C(44)−C(45)	1.522(8)
C(25)−C(26)	1.384(7)	C(45)−C(46)	1.511(7)
C(26)−C(27)	1.385(7)	C(46)−N(4)	1.470(6)
Pd(2)−Cl(2)−Pd(2A)	92.96(4)	C(24)−C(29)−P(2)	113.8(3)
Cl(2A)−Pd(2)−Cl(2)	87.04(4)	C(29)−P(2)−N(3)	99.6(2)
N(3)−Pd(2)−Cl(2)	95.27(11)	P(2)−N(3)−Pd(2)	109.77(19)
N(3)−Pd(2)−C(24)	84.09(16)	Pd(2)−N(3)−C(42)	126.7(3)
C(24)−Pd(2)−Cl(2A)	93.38(13)	N(3)−C(42)−O(2)	122.6(4)
C(25)−C(24)−Pd(2)	126.2(3)	N(3)−C(42)−N(4)	115.4(4)
Pd(2)−C(24)−C(29)	115.7(3)	C(42)−N(3)−P(2)	118.0(3)

1a−**f**, we have performed theoretical calculations of the mechanism of the palladation reaction using simplified model complexes. Therefore, all stabilized iminophosphoranes $R_3P{=}NC(O)Aryl$ have been represented by the ligand $PhH_2P{=}NC(O)C_6H_5$. The complete exploration of the potential energy surface was performed using quantum mechanics (QM) calculations (DFT at the B3LYP level).[22,23] Test calculations using the quantum mechanics/molecular mechanics (QM/MM) methodology ONIOM (B3LYP/UFF) were also performed using the actual ligand $Ph_3P{=}NC(O)Ph$ to check the accuracy of the model (Supporting Information). Solvent effects were taken into account by means of a continuum description of the solvent with the CPCM method.[24] The mechanism of the cyclopalladation of amines has been studied by DFT methods.[25] We have successfully used this mechanism to explain the behavior of nonstabilized iminophosphoranes $R_3P{=}NCH_2Aryl$,[6] and we have assumed here an identical pathway. It includes a six-membered transition state, analogous to other structures previously proposed on the basis of experimental results[16,26] and also similar to other TS described for related systems.[27]

The energy profile for the exo palladation of the model ligand $PhH_2P{=}NC(O)C_6H_5$ (Figure 4) shows the same steps as those described previously.[6,25a] After the initial N bonding of the

(20) (a) Pearson, R. G. *Inorg. Chem.* **1973**, *12*, 712. (b) Vicente, J.; Arcas, A.; Bautista, D.; Jones, P. G. *Organometallics* **1997**, *16*, 2127. (c) Vicente, J.; Abad, J. A.; Frankland, A. D.; Ramírez de Arellano, M. C. *Chem. Eur. J.* **1999**, *5*, 3066. (d) Vicente, J.; Abad, J. A.; Martínez-Viviente, E.; Jones, P. G. *Organometallics* **2002**, *21*, 4454.

(21) (a) Anderson, C.; Crespo, M. *J. Organomet. Chem.* **2004**, *689*, 1496. (b) Anderson, C.; Crespo, M.; Font−Bardía, M.; Klein, A.; Solans, X. *J. Organomet. Chem.* **2000**, *601*, 22.

(22) Frisch, M. J.; Trucks, G. W.; Schlegel, H. B.; Scuseria, G. E.; Robb, M. A.; Cheeseman, J. R.; Montgomery, J. A., Jr.; Vreven, T.; Kudin, K. N.; Burant, J. C.; Millam, J. M.; Iyengar, S. S.; Tomasi, J.; Barone, V.; Mennucci, B.; Cossi, M.; Scalmani, G.; Rega, N.; Petersson, G. A.; Nakatsuji, H.; Hada, M.; Ehara, M.; Toyota, K.; Fukuda, R.; Hasegawa, J.; Ishida, M.; Nakajima, T.; Honda, Y.; Kitao, O.; Nakai, H.; Klene, M.; Li, X.; Knox, J. E.; Hratchian, H. P.; Cross, J. B.; Bakken, V.; Adamo, C.; Jaramillo, J.; Gomperts, R.; Stratmann, R. E.; Yazyev, O.; Austin, A. J.; Cammi, R.; Pomelli, C.; Ochterski, J. W.; Ayala, P. Y.; Morokuma, K.; Voth, G. A.; Salvador, P.; Dannenberg, J. J.; Zakrzewski, V. G.; Dapprich, S.; Daniels, A. D.; Strain, M. C.; Farkas, O.; Malick, D. K.; Rabuck, A. D.; Raghavachari, K.; Foresman, J. B.; Ortiz, J. V.; Cui, Q.; Baboul, A. G.; Clifford, S.; Cioslowski, J.; Stefanov, B. B.; Liu, G.; Liashenko, A.; Piskorz, P.; Komaromi, I.; Martin, R. L.; Fox, D. J.; Keith, T.; Al-Laham, M. A.; Peng, C. Y.; Nanayakkara, A.; Challacombe, M.; Gill, P. M. W.; Johnson, B.; Chen, W.; Wong, M. W.; González, C.; Pople, J. A. Gaussian 03, Revision D.01; Gaussian, Inc., Wallingford, CT, 2004.

(23) (a) Becke, A. D. *J. Chem. Phys.* **1993**, *98*, 5648. (b) Lee, C.; Yang, W.; Parr, R. G. *Phys. Rev. B* **1988**, *37*, 785. (c) Stephens, P. J.; Delvin, F. J.; Chabalowski, C. F.; Frisch, M. J. *J. Phys. Chem.* **1994**, *98*, 11623.

(24) (a) Tomasi, J.; Persico, M. *Chem. Rev.* **1994**, *94*, 2027. (b) Amovilli, C.; Barone, V.; Cammi, R.; Cancès, E.; Cossi, M.; Mennucci, B.; Pomelli, C. S.; Tomasi, J. *Adv. Quantum Chem.* **1998**, *32*, 227. (c) Tomasi, J.; Mennucci, B.; Cammi, R. *Chem. Rev.* **2005**, *105*, 2999.

(25) (a) Davies, D. L.; Donald, S. M. A.; Macgregor, S. A. *J. Am. Chem. Soc.* **2005**, *127*, 13754. (b) Davies, D. L.; Donald, S. M. A.; Al-Duaij, O.; Macgregor, S. A.; Pölleth, M. *J. Am. Chem. Soc.* **2006**, *128*, 4210. (c) Ziatdinov, V. R.; Oxgaard, J.; Mironov, O. A.; Young, K. J. H.; Goddard, W. A., III; Periana, R. A. *J. Am. Chem. Soc.* **2006**, *128*, 7404.

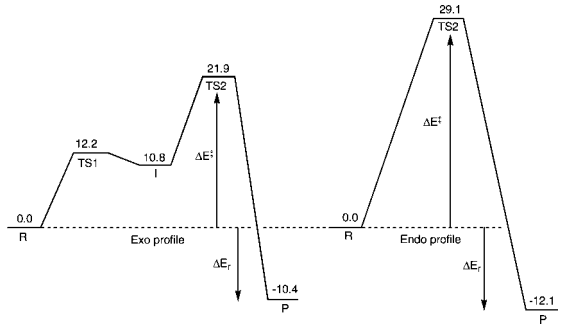

Figure 4. Computed reaction profiles (kcal/mol) for the exo and endo C−H bond activation of **1a** in CH_2Cl_2 as solvent. The zero energy point has been taken at the [Pd(κ^2-OAc)(κ^1-OAc)(κ^1-N-ligand)] species.

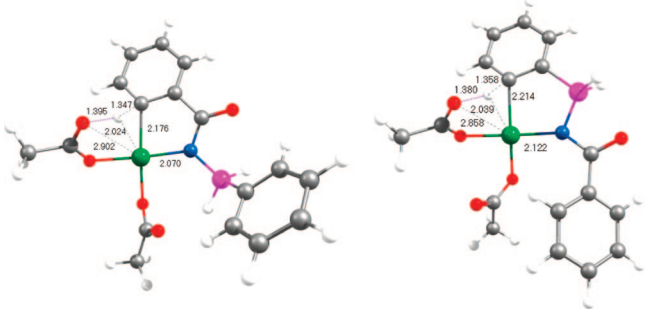

Figure 5. Computed structures for the **TS2** of exo (left) and endo (right) palladations of PhH_2P = NC(O)C_6H_5. Distances in Å.

Table 5. Activation Barriers ($\Delta E^{\ddagger}$) and Reaction Energies (ΔE_r) for the Exo and Endo Reaction Pathways in the Gas Phase and in Different Solvents[a]

	gas		dcm		tol	
	exo	endo	exo	endo	exo	endo
$\Delta E^{\ddagger}$	24.0	32.8	21.9	29.1	22.2	36.6
ΔE_r	−7.9	−11.5	−10.4	−12.1	−10.4	−13.3

[a] Energies are given in kcal/mol.

iminophosphorane (**R**_exo, Supporting Information) an agostic intermediate (**I**_exo) is reached through a first transition state (**TS1**_exo). The actual activation barrier $\Delta E^{\ddagger}$ is that defined by the transition state **TS2** (Figure 5, Table 5), which accounts for the proton migration from the aryl carbon to one oxygen atom of an acetate ligand. The ortho-palladated product **P**_exo (Supporting Information) is obtained after complete proton transfer and stabilization through the formation of an hydrogen bond. The energy profile of the endo palladation of PhH_2P═NC(O)C_6H_5 is also shown in Figure 4. In this case only the **TS2** is found (Figure 4, Table 5), in spite of intense research on the region where the plausible agostic intermediate is thought to be found, and thus the energy profile is simpler than that observed for the exo metalation.

The values shown in Table 5 (those in Figure 4 are calculated in CH_2Cl_2 as solvent) imply two significant facts. The first one is that the endo palladation is thermodynamically favored (ΔE_r) over the exo process, either in the gas phase or in a solvent

Scheme 3. Decomposition of the Activation Barrier (AB)

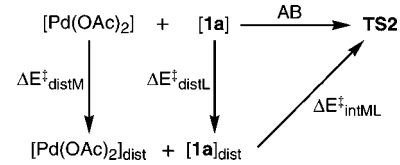

(CH_2Cl_2 or toluene). The second, more interesting, fact is that the activation barrier, determined by the $\Delta E^{\ddagger}$ value (Table 5), shows clearly that the reaction is kinetically controlled, since the values for the exo palladation are always substantially lower than those calculated for the endo process. The values of $\Delta E^{\ddagger}$ in CH_2Cl_2 (20−22 kcal/mol) are similar to those previously found in related systems[6] and seem to be easily reachable. In fact, the reactions take place in refluxing CH_2Cl_2. However, the values calculated for the endo pathway are notably higher (up to 7 kcal/mol) and seem to be unreachable. All attempts at ortho palladation in refluxing toluene were unsuccessful, and only decomposition was observed in all cases. The good agreement between the experimental facts and the calculated values ($\Delta E^{\ddagger}$ and ΔE_r) for the mechanism described here allow us to propose that the kinetic control of the reaction is the main reason for the regioselective ortho palladation of stabilized iminophosphoranes.

We have also performed calculations considering the complete model. The palladation of Ph_3P═NC(O)Ph with $Pd(OAc)_2$ has been studied using the QM/MM methodology. Complete details are given in the Supporting Information. The calculated gas-phase barriers for the model and real ligands differ by less than 1 kcal/mol. The QM/MM study on the real system provides the same conclusions as those described for the simplified model: (i) the reaction is kinetically controlled and favors the exo metalation; (ii) the endo products are thermodynamically more stable. Therefore, we will refer in the following paragraphs to the simplified model.

The small differences obseved in the stabilization energies (ΔE_r) between the endo and the exo metalations could be attributed to the endo effect. This effect may be responsible for the higher stabilization of the endo metalated derivatives with respect to the exo complexes.[7,8] However, the ultimate reasons that could account for the $\Delta E^{\ddagger}$ values at the **TS2** are not so straightforward and, since this seems to be the key step of the cyclopalladation reaction, we have attempted an analysis of the different components of the energy barrier. Similar analyses have been recently reported in discussions of the reactivity of the Pd center toward σ(C−H) and σ(C−X) bonds.[28] The formation of the **TS2**-exo and **TS**-endo states could be attained from the interaction of the $Pd(OAc)_2$ moiety and the PhH_2P═NC(O)C_6H_5 ligand when they are infinitely apart (Scheme 3), and this is the activation barrier of the process (AB in Scheme 3). This energy can be decomposed into three energies, two of them accounting for the distortions of the ligand PhH_2P═NC(O)C_6H_5 and the metallic fragment $Pd(OAc)_2$ from their isolated geometries to their distorted geometries in **TS2** ($\Delta E^{\ddagger}_{distL}$ for the ligand and $\Delta E^{\ddagger}_{distM}$ for the Pd fragment) and the other one being the interaction energy of the distorted fragments in the transition state ($\Delta E^{\ddagger}_{intML}$). The values are collected in Table 6.

These values show that the distortion energies are quite different in the two cases: 54.0 kcal/mol for the endo process and 63.5 kcal/mol for the exo reaction. The endo palladation

(26) (a) Ryabov, A. D.; Sakodinskaya, A. K.; Yatsimirsky, A. K. *J. Chem. Soc., Dalton Trans.* **1985**, 2629. (b) Kurzeev, S. A.; Kazankov, G. M.; Ryabov, A. D. *Inorg. Chim. Acta* **2002**, *340*, 192.

(27) (a) García-Cuadrado, D.; Braga, A. A. C.; Maseras, F.; Echavarren, A. M. *J. Am. Chem. Soc.* **2006**, *128*, 1066. (b) Lafrance, M.; Fagnou, K. *J. Am. Chem. Soc.* **2006**, *128*, 16496. (c) Lafrance, M.; Rowley, C. N.; Woo, T. K.; Fagnou, K. *J. Am. Chem. Soc.* **2006**, *128*, 8754.

(28) (a) Bickelhaupt, F. M. *Comput. Chem.* **1999**, *20*, 114. (b) Bickelhaupt, F. M.; Diefenbach, A. *J. Phys. Chem. A* **2004**, *108*, 8460. (c) Pierrefixe, S. C. A. H.; Bickelhaupt, F. M. *Chem. Eur. J.* **2007**, *13*, 6321.

Table 6. Decomposition of the Solvent-Phase Energy Barriers Calculated Following Scheme 3[a]

	$\Delta E^{\ddagger}_{distL}$	$\Delta E^{\ddagger}_{distM}$	$\Delta E^{\ddagger}_{intML}$
endo	38.6	15.4	−24.9
exo	36.0	27.5	−41.6

[a] The solvent is CH_2Cl_2. Energies are given in kcal/mol.

implies a more flexible $NP(H)_2Ph$ fragment, while the exo process implies a delocalized planar, more rigid NC(O)Ph moiety. Nevertheless, endo palladation should be favored, since less energy would be implied. Where is the difference? The critical point comes from the calculated values of the interaction energies. In fact, there is a much higher release of energy as a consequence of the interaction of the distorted fragments in the exo than in the endo case (−41.6 vs −24.9 kcal/mol). This large difference (16.7 kcal/mol) counterbalances the differences in distortion energies (9.5 kcal/mol) and gives a net balance of 7.2 kcal/mol in favor of the exo activation barrier. We believe therefore that the ultimate reason for the regioselectivity found is the strength of the metal−ligand interaction at the transition state **TS2**, and we have demonstrated that in the exo pathway this interaction is stronger. A careful inspection of the calculated **TS2** structures (Figure 5) provides additional information. The exo structure shows a Pd−C bond distance (2.176 Å) shorter than that found in the endo structure (2.214 Å), pointing again to a stronger bond in the former case. In addition, the exo structure shows the presence of a strong hydrogen bond (O···H = 2.136 Å) between the nonbonded oxygen of the acetate ligand cis to the iminic N atom and one ortho H atom of the C_6H_5 group linked to the P atom. In the endo structure there is also a hydrogen bond between the same oxygen and the ortho proton of the $C(O)C_6H_5$ group, but this H bond should be weaker, since the O···H distance is 2.390 Å. These two facts—the different strengths of the Pd−C interaction and the presence of H bonds of different intensity involving one acetate and the phenyl unit not involved in the palladation—seem to be at the origin of the higher release of energy in the exo as compared to that in the endo processes and, consequently, at the origin of the lower activation barrier for the exo metalation.

Conclusion

The ortho metalation of stabilized iminophosphoranes $R_3P{=}NC(O)Aryl$ with $Pd(OAc)_2$ takes place regioselectively at the aryl ring of the benzamide group, giving five-membered exo palladacycles of high stability, through a $C(sp^2)$−H bond activation process. The presence of different substituents does not alter the reaction orientation. Similar observations apply in the formation of six-membered palladacycles or when bisphosphine derivatives $Ph_2P(CH_2)_nPPh_2$ are used. This general trend is only inverted when a $C(sp^3)$−H bond activation is considered, and endo palladations are obtained instead. DFT calculations (B3LYP level) on the mechanism of this cyclopalladation reaction show that the process is kinetically controlled. The lower energy of the transition states of the exo pathways are due to a stronger interaction of the aryl ring to be palladated with the Pd center and also to the presence of stronger H bonds between the acetate ligand trans to the palladated position and the phenyl ring not involved in the palladation process.

Experimental Section

Caution! The organic azides are *highly hazardous* materials which can explode and whose preparation and manipulation must be carried out with maximum caution. They must be stored at low temperature ($T \approx 0$ °C) and dissolved in an inert solvent.[11]

General Methods. General methods are as reported elsewhere.[4–6] **1a**−**c** were prepared following reported procedures by Pomerantz et al.[9] **1d**−**I** were obtained through the Staudinger method (see the Supporting Information).[10] The azides $N_3C(O)CH_2C_6H_5$ $N_3C(O)C_6H_5$, $N_3C(O)NC_4H_8$, $N_3C(O)NC_4H_8O$, $N_3C(O)$-2-C_4H_3O, and $N_3C(O)$-2-C_4H_3S were synthesized according to published methods.[11]

[Pd(*μ*-Cl){C_6H_4(C(O)N=P(*p*-tol)$_3$-*κC*,*N*)-2}]$_2$ (2a). A solution of $Pd(OAc)_2$ (0.076 g, 0.342 mmol) and **1a** (0.145 g, 0.342 mmol) in CH_2Cl_2 (20 mL) was refluxed for 2.5 h. After this time, some decomposition was evident. The black suspension was treated with charcoal (15 min) and then filtered through a Celite pad. The orange solution, which contained the acetate intermediate, was evaporated to dryness and the residue dissolved in 20 mL of MeOH. The resulting clear solution was treated with an excess of anhydrous LiCl (0.206 g, 4.86 mmol), resulting in the precipitation of **2a** (0.037 g, 19.2%) as a yellow solid, which was filtered, washed with MeOH (5 mL) and Et_2O (20 mL), and dried under vacuum. Anal. Calcd for $C_{56}H_{50}Cl_2N_2O_2P_2Pd_2$ (1128.2): C, 59.57; H, 4.46; N, 2.48. Found: C, 59.27; H, 4.41; N, 1.95. IR: ν 1644 ($\nu_{C=O}$), 1295 ($\nu_{P=N}$) cm^{-1}. ^1H NMR (400 MHz, CD_2Cl_2): δ 2.28 (s, 9H, Me, P(*p*-tol)$_3$), 6.62 (m, 1H, C_6H_4), 6.76 (m, 1H, C_6H_4), 6.86 (m, 1H, C_6H_4), 7.01 (m, 1H, C_6H_4), 7.21 (m, 6H, H_m, P(*p*-tol)$_3$), 7.78 (m, 6H, H_o, P(*p*-tol)$_3$). $^{13}C\{^1H\}$ NMR ($CDCl_3$): δ 21.75 (s, Me, P(*p*-tol)$_3$), 122.31 (d, $^1J_{PC}$ = 104.5 Hz, C_i, P(*p*-tol)$_3$), 123.78 (s, C_6H_4), 127.80 (d, $^3J_{PC}$ = 2.8 Hz, C_6H_4), 129.39 (d, $^3J_{PC}$ = 13.4 Hz, C_m, P(*p*-tol)$_3$), 129.54 (s, C_6H_4), 133.58 (s, C_6H_4), 133.76 (d, $^2J_{PC}$ = 10.5 Hz, C_o, P(*p*-tol)$_3$), 139.74 (d, $^3J_{PC}$ = 14.0 Hz, C_2, C_6H_4), 143.28 (s, C_1, C_6H_4), 143.44 (d, $^3J_{PC}$ = 2.4 Hz, C_p, P(*p*-tol)$_3$), 180.89 (d, $^2J_{PC}$ = 5.4 Hz, CO). $^{31}P\{^1H\}$ NMR (CD_2Cl_2): δ 29.31. MS (FAB+): *m*/*z* (%) 1130 (92) $[M + H]^+$.

The syntheses of complexes **2b**,**c**,**e**−**h** are similar to that described for **2a** and (see the Supporting Information).

[Pd(*μ*-Cl){C_6H_4(CH_2C(O)N=PPh$_3$-*κC*,*N*)-2}]$_2$ (2d). To a solution of $Li_2[PdCl_4]$ (0.132 g, 0.506 mmol) in a MeOH/CH_2Cl_2 mixture (1/10, 22 mL) was added compound **1d** (0.200 g, 0.506 mmol), and the resulting mixture was stirred overnight (12 h) at 25 °C. After the reaction had taken place, the orange solution was evaporated to a small volume (~2 mL). Further stirring gave **2d** (0.212, 73.3%) as a yellow solid, which was filtered, washed with MeOH (2 mL) and Et_2O (20 mL), and dried under vacuum. Complex **2d** was characterized (NMR) as a mixture of trans and cis isomers in a 7/1 molar ratio. Anal. Calcd for $C_{52}H_{42}Cl_2N_2O_2P_2Pd_2$ (1072.1): C, 58.20; H, 3.94; N, 2.61. Found: C, 58.39; H, 3.84; N, 2.76. IR: ν 1629 ($\nu_{C=O}$), 1333 ($\nu_{P=N}$) cm^{-1}. ^1H NMR (400 MHz, $CDCl_3$): δ 5.01 (d, major, $^2J_{HH}$ = 16.4 Hz, CH_2), 5.12 (d, major, CH_2), 5.30 (d, minor, $^2J_{HH}$ = 16.6 Hz, CH_2), 5.43 (d, minor, $^2J_{HH}$ = 16.6 Hz, CH_2) 6.97 (d, major, $^3J_{HH}$ = 7.1 Hz, C_6H_4), 7.09−7.13 (m, C_6H_4), 7.19 (t, major, $^3J_{HH}$ = 7.6 Hz, C_6H_4), 7.32−7.39 (m, both, H_m, PPh_3), 7.60 (m, both, H_p, PPh_3), 7.83−7.88 (m, both, H_o, PPh_3). $^{31}P\{^1H\}$ NMR ($CDCl_3$): δ 37.54 (major), 37.87 (minor). MS (FAB+): *m*/*z* (%) 500 (30) $[M/2 - Cl]^+$.

[Pd{C_6H_4(C(O)N=P(*p*-tol)$_3$-*κC*,*N*)-2}(acac-*O*,*O*′)] (3a). To a solution of complex **2a** (0.045 g, 0.040 mmol) in CH_2Cl_2 (20 mL) was added Tl(acac) (0.024 g, 0.080 mmol), and the resulting suspension was stirred at 25 °C for 1 h. After the reaction had taken place, the suspension was filtered through a Celite pad, and the resulting solution was evaporated to dryness. Treatment of the oily residue with cold *n*-hexane (15 mL) gave **3a** (0.026 g, 52.5%) as a white solid. Anal. Calcd for $C_{33}H_{32}NO_3PPd$ (627.7): C, 63.09; H, 5.13; N, 2.23. Found: C, 62.83; H, 5.29; N, 2.03. IR: ν 1635 ($\nu_{C=O}$), 1589 (ν_{acac}), 1516 (ν_{acac}), 1291 ($\nu_{P=N}$) cm^{-1}. ^1H NMR (400 MHz, $CDCl_3$): δ 1.07 (s, 3H, Me, acac), 1.97 (s, 3H, Me, acac), 2.39 (s, 9H, Me, P(*p*-tol)$_3$), 5.02 (s, 1H, CH, acac), 7.01 (t, 1H, $^3J_{HH}$ = 7.3 Hz, H_4, C_6H_4), 7.16 (td, 1H, $^3J_{HH}$ = 7.3, $^4J_{HH}$ = 1.1

Hz, H_5, C_6H_4), 7.23 (m, 6H, H_m, P(*p*-tol)$_3$), 7.31 (dd, 1H, $^3J_{HH}$ = 7.5, $^4J_{HH}$ = 1.6 Hz, H_3, C_6H_4), 7.59 (d, 1H, $^3J_{HH}$ = 7.6 Hz, H_6, C_6H_4), 7.88 (m, 6H, H_o, P(*p*-tol)$_3$). $^{13}C\{^1H\}$ NMR ($CDCl_3$): δ 21.69 (s, Me, P(*p*-tol)$_3$), 26.39 (s, Me, acac), 27.47 (s, Me, acac), 99.17 (s, CH, acac), 122.94 (d, $^1J_{PC}$ = 104.7 Hz, C_i, P(*p*-tol)$_3$), 124.00 (s, C_6H_4), 127.37 (d, J_{PC} = 3.2 Hz, C_6H_4), 129.00 (s, C_6H_4), 129.12 (d, $^3J_{PC}$ = 13.4 Hz, C_m, P(*p*-tol)$_3$), 130.10 (s, C_6H_4), 133.52 (d, $^2J_{PC}$ = 10.6 Hz, C_o, P(*p*-tol)$_3$), 140.55 (d, $^3J_{PC}$ = 13.6 Hz, C_2, C_6H_4), 143.08 (d, $^4J_{PC}$ = 2.9 Hz, C_p, P(*p*-tol)$_3$), 146.50 (s, C_1, C_6H_4), 181.06 (d, $^2J_{PC}$ = 5.3 Hz, CO), 186.40 (s, CO, acac), 186.27 (s, CO, acac). $^{31}P\{^1H\}$ NMR ($CDCl_3$): δ 28.04. MS (FAB+): *m/z* (%) 628 (30) $[M]^+$.

The syntheses of complexes **3b**−**d** are similar to that described for **3a** (see the Supporting Information).

***trans*-[PdCl$_2${N(PPh$_3$)C(O)CH$_2$Ph}$_2$] (4).** To a solution of **1d** (0.178 g, 0.452 mmol) in CH_2Cl_2 (10 mL) was added $Pd(OAc)_2$ (0.101 g, 0.452 mmol), and the resulting mixture was refluxed for 2 h. The resulting orange yellowish solution was evaporated to dryness, the yellow residue was dissolved in MeOH (15 mL), and this solution was treated with LiCl (0.153 g, 3.610 mmol). Further stirring at 25 °C gave **4** (0.098 g, 44.7%) as a yellow solid. Anal. Calcd for $C_{52}H_{44}Cl_2N_2O_2P_2Pd$ (967.7): C, 64.48; H, 4.58; N, 2.89. Found: C, 64.38; H, 4.69; N 2.85. IR: ν 1621 ($\nu_{C=O}$), 1339 ($\nu_{P=N}$) cm^{-1}. ^1H NMR (400 MHz, $CDCl_3$): δ 3.82 (s, 2H, CH_2), 6.90 (d, 2H, $^3J_{HH}$ = 6.8 Hz, H_o, Ph), 7.05 (m, 1H, H_p, Ph), 7.12 (m, 2H, H_m, Ph), 7.19−7.32 (m, 9H, H_o, H_p, PPh_3), 7.79 (m, 6H, H_m, PPh_3). $^{13}C\{^1H\}$ NMR ($CDCl_3$): δ 45.97 (d, $^2J_{PC}$ = 3.4 Hz, CH_2), 125.98 (s, C_p, Ph), 127.89 (s, C_m, Ph), 128.61 (d, $^2J_{PC}$ = 13.3 Hz, C_m, PPh_3), 130.43 (s, C_o, Ph), 131.96 (d, $^4J_{PC}$ = 2.7 Hz, C_p, PPh_3), 132.64 (s, broad, C_o, PPh_3), 136.39 (d, $^4J_{PC}$ = 2.3 Hz, C_i, Ph), 183.13 (d, $^2J_{PC}$ = 5.2 Hz, CO) (signals assigned to the C_i of the PPh_3 group were not detected). $^{31}P\{^1H\}$ NMR ($CDCl_3$): δ 35.38 MS (FAB+): *m/z* (%) 967 (3) $[M]^+$, 931 (75) $[M - Cl]^+$.

Computational Details. Calculations were performed using the *Gaussian03* series of programs.[22] The reaction mechanism of the palladation of $PhH_2P{=}NC(O)C_6H_5$ (simplified model for reactants **R**, transition states **TS**, and products **P** of the endo and exo pathways) was studied using density functional theory (DFT) with the B3LYP functional.[23] In all cases, effective core potentials (ECP) were used to represent the innermost electrons of the palladium atom.[23,29] The basis set for Pd was that associated with the pseudopotential with a standard double-ζ LANL2DZ contraction.[22] The C, N, O, and P atoms were represented by means of the 6-31G(d) basis set, whereas the 6-31G basis set was employed for the H atoms.[30] All geometry optimizations were full, with no restrictions. Stationary points located in the potential energy hypersurface were characterized as true minima or transition states through vibrational analysis. Solvent effects were taken into account by means of C-PCM[11] using standard options. Free energies of solvation were calculated with toluene (ϵ = 2.38) and CH_2Cl_2 (ϵ = 8.93) as solvents, keeping the geometry optimized for the gas-phase species.

X-ray Crystallography. Crystals of **2b**,**g** and **3a** of quality sufficient for X-ray measurements were grown by vapor diffusion of Et_2O into CH_2Cl_2 (**2b**, **3a**) or $CHCl_3$ (**2g**) solutions of the crude products at 25 °C. In each case, a single crystal was mounted at the end of a quartz fiber in a random orientation, covered with perfluorinated oil, and placed under a cold stream of N_2 gas. Data collections were performed on Bruker Smart Apex CCD and Oxford Diffraction Xcalibur2 diffractometers using graphite-monocromated Mo Kα radiation (λ = 0.710 73 Å). In all cases, a hemisphere of data was collected on the basis of ω-scan and ϕ-scan runs. The diffraction frames were integrated using the programs SAINT[31] and CrysAlis RED,[32] and the integrated intensities were corrected for absorption with SADABS.[33] The structures were solved and developed by Fourier methods.[34] All non-hydrogen atoms were refined with anisotropic displacement parameters. The H atoms were placed at idealized positions and treated as riding atoms. Each H atom was assigned an isotropic displacement parameter equal to 1.2 times the equivalent isotropic displacement parameter of its parent atom. The structures were refined to F_o^2, and all reflections were used in the least-squares calculations.[35]

Acknowledgment. Funding by the Ministerio de Educación y Ciencia (MEC) (Spain, Projects CTQ2005-01037 and CTQ2005-09000-C02-01) is gratefully acknowledged. R.B. (BES2003-0296) and D.A. thank the MEC (Spain) and Diputación General de Aragón (Spain) for respective Ph.D. research grants.

Supporting Information Available: Text giving the complete experimental section with all preparative data and figures and tables giving complete data collection parameters for **2b**, **3a**, and **2g**·$CHCl_3$ and Cartesian coordinates of reagents (**R**), transition states (**TS**), and ortho-metalated products (**P**) for the endo and exo palladation of $PhH_2P{=}NC(O)Ph$ and $Ph_3P{=}NC(O)Ph$. This material is available free of charge via the Internet at http://pubs.acs.org.

OM701174V

(29) Hay, P. J.; Wadt, W. R. *J. Chem. Phys.* **1985**, *82*, 299.

(30) (a) Hehre, W. J.; Ditchfield, R.; Pople, J. A. *J. Phys. Chem.* **1972**, *56*, 2257. (b) Hariharan, P. C.; Pople, J. A. *Theor. Chim. Acta* **1973**, *28*, 213. (c) Francl, M. M.; Pietro, W. J.; Hehre, W. J.; Binkley, J. S.; Gordon, M. S.; DeFrees, D. J.; Pople, J. A. *J. Chem. Phys.* **1982**, *77*, 3654.

(31) SAINT, version 5.0(31); Bruker Analytical X-ray Systems, Madison, WI.

(32) CrysAlis RED, version 1.171.27p8; Oxford Diffraction Ltd., Oxford, U.K., 2005.

(33) Sheldrick, G. M. SADABS, Program for Absorption and Other Corrections; University of Göttingen, Göttingen, Germany, 1996.

(34) Sheldrick, G. M. SHELXS-86. *Acta Crystallogr.* **1990**, *A46*, 467.

(35) Sheldrick, G. M. SHELXL-97: FORTRAN Program for the Refinement of Crystal Structures from Diffraction Data; University of Göttingen, Göttingen, Germany, 1997. Molecular graphics were done using the following commercial package: SHELXTL-PLUS, Release 5.05/V; Siemens Analytical X-ray Instruments, Inc., Madison, WI, 1996.